

# **Microdevice Enabling Long-term in Vitro Study of Biofabricated Constructs**

A Technical Report submitted to the Department of Biomedical Engineering

Presented to the Faculty of the School of Engineering and Applied Science

University of Virginia • Charlottesville, Virginia

In Partial Fulfillment of the Requirements for the Degree

Bachelor of Science, School of Engineering

**Joshua Goedert**

Spring, 2023

Technical Project Team Members

Alex Burnside

On my honor as a University Student, I have neither given nor received unauthorized aid on this assignment as defined by the Honor Guidelines for Thesis-Related Assignments

Chris Highley, Department of Biomedical Engineering and Chemical Engineering

# Microdevice Enabling Long-Term in Vitro Studies of Biofabricated Constructs

Joshua A. Goedert<sup>a</sup>, Alexandra L. Burnside<sup>b</sup>, Christopher B. Highley<sup>c,1</sup>

<sup>a</sup> University of Virginia, Undergraduate Biomedical Engineering

<sup>b</sup> University of Virginia, Undergraduate Biomedical Engineering

<sup>c</sup> University of Virginia, PhD. Biomedical Engineering

<sup>1</sup> Correspondence: University of Virginia Biomedical Engineering Department

## **Abstract**

Within the field of biomedical engineering, hydrogels have numerous applications, such as drug delivery vectors, biosensors, and tissue engineering scaffolds (Chai et al., 2017). However, traditional hydrogels have limitations in terms of cell motility, tissue morphogenesis, and control over material properties. Granular hydrogels, composed of hydrogel microparticles (HMPs), have emerged as a promising alternative due to their injectable, self-assembling, shear-thinning, and self-healing properties. Inherent porosity within granular hydrogels allows for the rapid exchange of reactants, nutrients, and waste, promoting cellular infiltration and subsequent tissue remodeling.

Despite their potential, granular hydrogels present challenges for long-term study in traditional cell culture due to their dynamic nature. To overcome this, our capstone project aims to design and prototype a microfluidics device using polydimethylsiloxane (PDMS) to maintain small amounts of granular hydrogels in cell culture over time. The PDMS microfluidics device described enables stable culture in granular hydrogel-based materials by securing the material and preventing the loss of material during cell culturing. This device is a crucial first step in fully utilizing granular hydrogel materials in the biomedical field, especially in tissue engineering research. By enabling long-term culture of granular hydrogels, this device will allow for the development of complex tissue and disease models, and provide insights into the behavior of cells in dynamic environments.

Keywords: Granular hydrogels, cell culture, PDMS, microdevice, tissue engineering, microgels

---

## **Introduction**

In the past few decades, the field of tissue engineering has rapidly advanced at the intersection of technology, biology, and materials science (Fisher & Mauck, 2013). The interdisciplinary field of tissue engineering aims to mimic the native biology found in the human body by creating functional living tissue. Tissue engineering typically focuses on replicating the complex functional and structural components of natural tissue such as biochemical cues, biomechanical cues, cellular organization, and the extracellular matrix. By mimicking native biology, tissue engineering aims to create tissue constructs that have the ability to integrate within host tissue and promote regular biological function.

Hydrogels are commonly used as biological scaffolds in tissue engineering due to their high water content that mimics native tissue. Their ability to absorb water is due to

the 3D networks of hydrophilic polymers. Hydrogels have various biomedical applications due to their water content, biocompatibility, biodegradability, mechanical properties, and tunable surface modifications (Bashir et al., 2020). The composition of hydrogels can vary immensely and their main constituents can be composed of materials such as collagen, alginate, polyethylene, and chitosan. The ability to construct hydrogels from synthetic and natural materials provides flexibility and allows for a broad range of applications. Their various adjustable properties also make them a suitable scaffold for cell culturing, enabling the recapitulation of the native environment.

Despite decades of research with hydrogel-based scaffolds, vascularization continues to be exceedingly difficult (Song et al., 2018). The complex interactions and self-organization that occur during neo-vascularization are not fully understood, making it challenging to design hydrogel-based

systems that can promote the formation of blood vessels. This difficulty leads to inadequate nutrient and oxygen supply to engineered tissues, limiting their growth and functionality. This is a critical issue in tissue engineering, as the lack of vascularization can lead to inadequate nutrient and oxygen supply to the engineered tissue, limiting its growth and functionality. Therefore, further research is needed to better understand the complex mechanisms involved in neo-vascularization and to develop innovative approaches to promote the formation of functional blood vessels within hydrogel-based tissue constructs. As a result, researchers have been striving to develop new strategies that can address issues regarding vascularization.

Additionally, hydrogel systems can reduce cell motility due to poor infiltration, which can further limit the functionality of engineered tissue constructs (Qazi & Burdick, 2021). The bulk nature of hydrogels can impede cell movement by acting as a physical barrier rather than allowing them to move through as they may in native tissue. This can lead to less cell-cell interaction and reduce tissue formed within these constructs. Furthermore, these physical limitations within the hydrogel can interfere with the cell's ability to form structures as the cells may not be able to create the necessary forces or undergo the shape changes required for tissue morphogenesis. Hydrogel systems may also lack the appropriate mechanical properties required for cell and tissue organization.

Granular hydrogels, however, may offer a solution to these problems. While traditional hydrogels, bulk hydrogels, are crosslinked together to form single, continuous features, granular hydrogels are made of hydrogel microparticles (HMPs) that are not crosslinked to each other. HMPs have several unique properties that can make them advantageous over bulk hydrogels for certain applications, including injectability, inherent porosity due to interstitial space between particles, shear-thinning behavior, and modularity due to the ability to mix particles of different sizes or compositions (Bashir et al., 2020). While maintaining the important properties of the hydrogel, such as high water content and ability to be modified, granular hydrogel materials are also inherently dynamic, so when used in cell culture the cells are able to move through the material. This allows for cells to migrate and form arrangements, creating vascularization and other complex structures.

However, the non-crosslinked nature of these microgels can be a limiting factor when used in cell culture. The hydrostatic pressures that occur during traditional cell culture techniques, especially during media exchange, can

cause the HMPs and their microstructures to erode. Additionally, these granular hydrogel materials are time-consuming and expensive to fabricate, so the loss of material in this way is a serious issue. As research with these HMP materials expands, the need for a device that can effectively contain the microgels and stabilize them for use in cell culture over a period of time is rapidly increasing. There is currently no standard method or device that accomplishes this goal, as most work to tackle this issue has been done on a very small scale, with the fabrication of singular devices intended for specific experiments.

This project set out to create a device capable of containing and stabilizing granular hydrogels during long term cell culture experiments. The first aim was to design, iterate upon, and fabricate this microdevice, using PDMS as the base material. The second aim was to use the base design from Aim 1 and begin to implement more complex design features, such as perfusion between wells. While Aim 2 was not completed in full, important steps were made to demonstrate the ability to construct more complex features within this base device and prove its viability to be further developed for use in more complex systems and applications.

## **Results**

### ***Design constraints***

To guide the design process, several constraints were initially identified. The most important considerations were that the device must maintain cell viability and it must contain the granular hydrogel material within a defined space during standard cell culture conditions. Additionally, it was decided that the device should be able to fit on a standard glass coverslip, approximately 25 mm x 76 mm.

### ***Final device design***

The final device design contains three separate wells and consists of four components: the base, lid, glass bottom, and mesh squares. These components fit together as shown in Figure 1. The base and lid are both made of PDMS. The mesh insert sits on top of the well, containing the material within the well, and is held in place by the lid. The lid has through channels above each well, allowing for media exchange to be performed during cell culture without removing the lid. In this way, the media can be introduced from the lid, it will pass through the mesh membrane, and waste and old media can be removed via aspiration through the lid while the mesh holds the granular hydrogel material in place. Each well has a volume of 180  $\mu\text{L}$ , and each

channel in the lid holds 250 $\mu$ L of media. The device all fits within the 25 mm x 76 mm dimensions of a glass coverslip and has a thickness of approximately 13 mm.

way through the base, which allowed us to bond a glass coverslip.

In the final few iterations, we refined the overall shape and

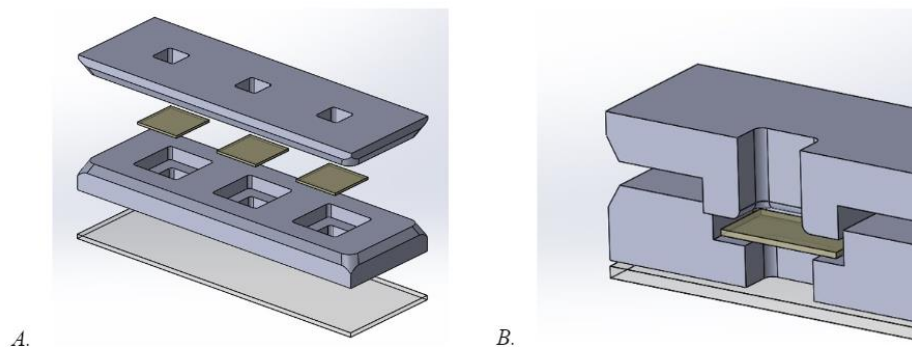


**Fig. 1. CAD renderings of the final device.** (A) Exploded view of the final design which includes the lid, mesh inserts, base, and glass coverslip. (B) Cross-sectional view of a single well, showing the interlocking lid and the compartments above and below the mesh for media and the material respectively.

### *Device iterations*

The first concept featured a smaller but thicker device, measuring roughly 16 mm x 40 mm x 20 mm (as seen in Fig S1). This model had only two wells, each comparable in volume to the final iteration. There was a slot between the wells with raised cylindrical protrusion on either end to prevent liquid from crossing between the wells. Unlike the final version, this iteration had no glass bottom, and the entire device, except for the mesh, was composed of PDMS. Furthermore, the lid was thinner but had raised edges around the through hole to hold approximately 160  $\mu$ L media.

In the following iterations, we optimized the design for the molding process by removing some small features from the first design, such as the thin edges around the top of the base and the raised edges around the through holes in the lid. This resulted in a more robust device that was less fragile when removing it from the mold. Other features, such as the slot and raised portions, were retained.

For the next iterations, we focused on minimizing the amount of material needed to make the device and improving key features. The overall dimensions were reduced while maintaining large enough features to improve the device removal process. Additionally, the edges of the device were chamfered to more easily remove the PDMS from the mold. In this version, the base had small insets that the lid would fit into instead of the slot and raised cylindrical protrusions. Finally, in this version, the wells went all the

fit of the lid onto the base. We also added an additional well to better utilize the surface area on the glass coverslip and allow for triplicates in experiments. The dimensions of the wells and through holes were finalized at approximately 180  $\mu$ L and 250  $\mu$ L, respectively. We tested various tolerances between the lid and base to find an optimal fit where a water-tight seal could be achieved.

### *Alternative designs*

While the final design for our device consisted of a three-welled rectangular shape that fit onto a standard glass coverslip, we tested other form factors. One of the alternative designs was a three-welled circular device that could fit into a standard 6-well plate. The three circular wells were arranged in a triangular formation to optimize the space between them. The volumes of both the base and lid were consistent with the final design. The rest of the device followed the general specifications of the final iteration, including the insets, through holes, and glass bottom. However, due to time constraints, we were unable to further test the prototype.

We also tried a different iteration of the final design that had a single channel running the length of the device, through each of the wells. Furthermore, this design had interlocking protrusions and corresponding slots on the ends of the device to allow multiple devices to be connected and extend the system. Otherwise, the device remained functionally equivalent to the final design. However, we were unable to test these functionalities or perfusion of the channel due to time limitations.

Finally, we designed a four-welled PDMS device that consisted of a 2x2 array of wells. There were a total of two channels in the device, which were arranged in a parallel configuration. One channel ran through the middle of two adjacent wells, while the other channel ran through the middle of the two wells beside it. This device was intended to showcase replicable bioprinting across multiple wells, the perfusion of channels, and the use of selective cross-linking. However, we were unable to perform these tests within the time frame of the project.

### *Dye test*

One of the preliminary tests conducted was a dye test to determine the device's ability to contain liquids within the wells. The objective was to test the bond between the base and glass coverslip, as well as the fit between the lid and the base. During the first trial, the wells were dry in less than an hour because the dye seeped between the base and glass. In the second trial, a new glass coverslip and base were bonded together, and the liquid in the wells was maintained for over five days. However, the dye was observed to seep between the base and lid during this time. While larger amounts of liquid were visible between the base and lid over the course of the five days, the liquid remained contained within the device.

### *Cell viability (without microgels)*

In order to assess the viability of cells in the device, fibroblast cells were seeded at a concentration of 10,000

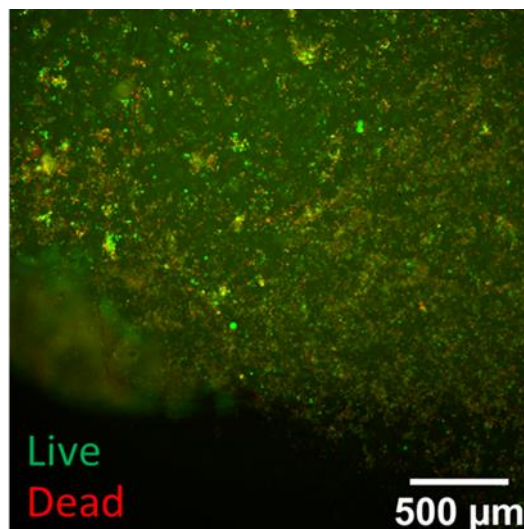


**Fig. 2. Cell viability assessment using LIVE/DEAD™ stain.** This fluorescence microscopy image shows a live dead stain of fibroblasts in the device where the green indicates the live cells and the red indicates the dead cells. The stain reveals the overall distribution of live and dead cells within the device.

cells per milliliter (10,000 cells/mL) into each well. After two days, a LIVE/DEAD™ stain was applied, and the wells were imaged at a 10x magnification (Figure 2). However, we encountered issues in accurately quantifying the number of live cells from the images obtained. The thresholding techniques used varied significantly and resulted in a wide range of results that we did not feel confident in reporting. Despite this, we chose to use the images as qualitative data

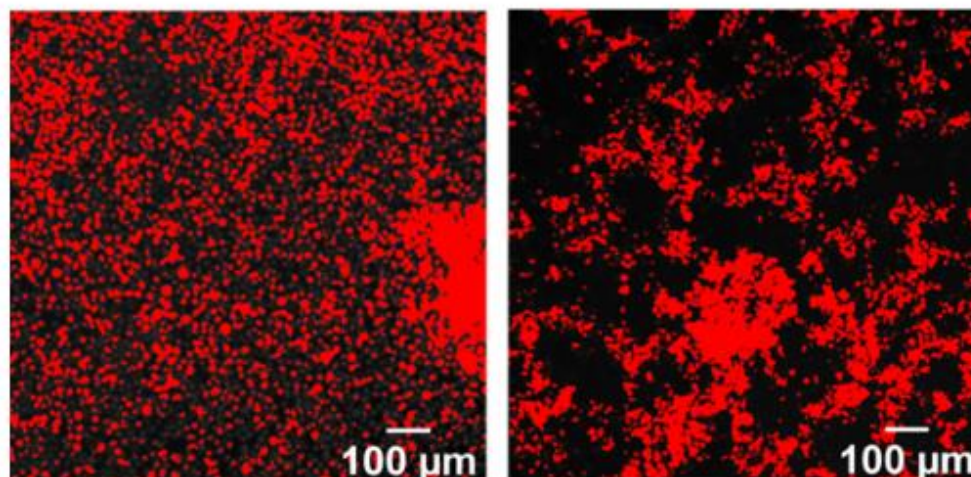


**Fig. 3. Formation of networks and cell aggregation.** This fluorescence microscopy image captures the development of cellular networks and the aggregation of human umbilical vein endothelial cells (HUVECs) over the course of 48 hours. The left image depicts the cells on day 0, while the right image showcases their structure on day 2. By utilizing the DsRed stain, we were able to visualize the dynamic interactions between the cells and their surrounding environment. This image offers insight into the dynamic behavior and organization of HUVECs in the device over time.



to demonstrate the precedence of viable cells within the device.

To further investigate the viability of cells within the device, human umbilical vein endothelial cells were seeded at 50,000 cells/mL and we conducted a second experiment using a DsRed stain over a two-day period. Since this stain

DAPI and Phalloidin to allow for imaging. The cells remained viable throughout this experiment, and the representative image in Figure 5 shows morphology changes, indicating that the cells were adherent and proliferating. The gradual loss of focus in the image suggests that the cells were interacting with the microgels in their environment in three dimensions. During one of the

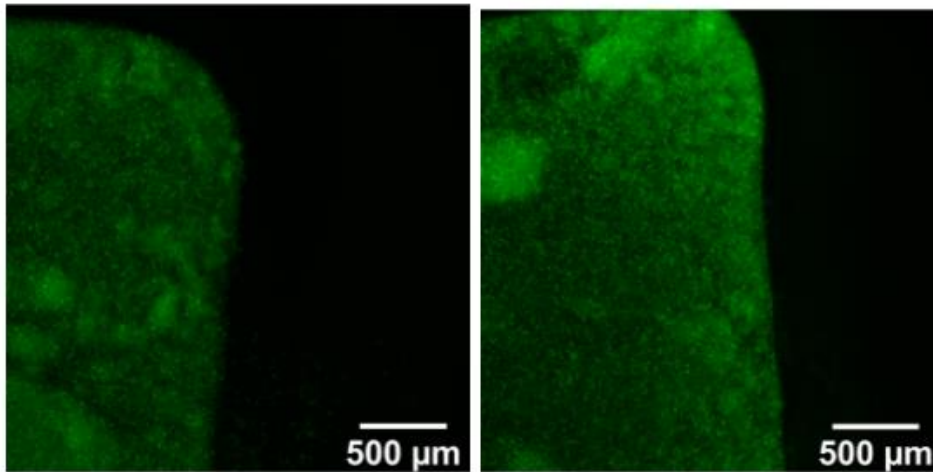


**Fig. 4. Microgels device.** This figure shows FITC tagged PEG granular hydrogels at day 0 (left) and day 2 (right) of encapsulation within the device during standard cell culture conditions.

does not damage cells, we were able to analyze changes over time. Figure 3 shows that on day 0, the cells were relatively dispersed with some clustering. However, on the second day, noticeable structural differences were observed, indicating that the cells had self-aggregated, started to form networks, and interacted with both each other and their environment.

#### ***Microgel encapsulation***

The most crucial aspect of the device was that it must contain granular hydrogels during standard cell culture conditions. This was tested by loading each well of a device with FITC-tagged PEG granular hydrogels that were mostly <40 µm in diameter. These wells were imaged at day 0, looking at the initial level of containment of microgels within the device wells, and at day two to determine if containment was successful over time. As Figure 4 shows, there is a very clear distinction at the border of the well, where there are no microgels beyond the limits of the well in the rest of the device.

#### ***Cell morphology***

To examine the interactions between cells and microgels within the device, HUVECs and PEG microgels were seeded into the wells of a device for a four-day long experiment. After day four, the cells were stained with

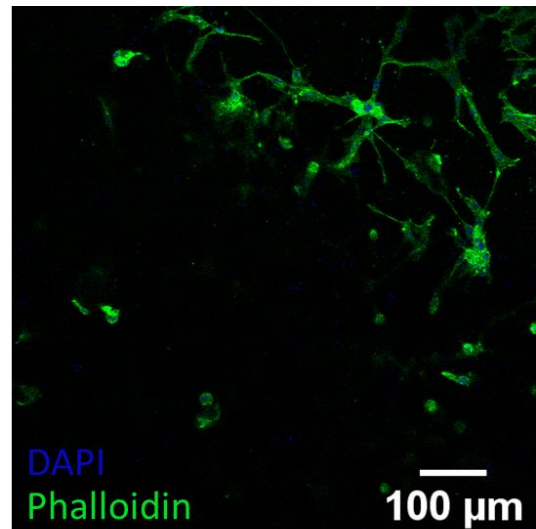


**Fig. 5. Visualization of fibroblast morphology changes within PEG microgel environment.** This fluorescence microscopy image at 20x magnification showcases live fibroblasts and their protrusions within PEG microgels. The fibroblasts, visible as elongated cells with nuclei stained with DAPI, are surrounded by the PEG microgels and have extended protrusions. The use of phalloidin staining facilitated the visualization of cellular protrusions.

media exchange aspirations, a mesh moved and had to be readjusted, but no adverse results were gathered as a result. There was no reported media loss throughout this experiment. The viability and morphology of the cells

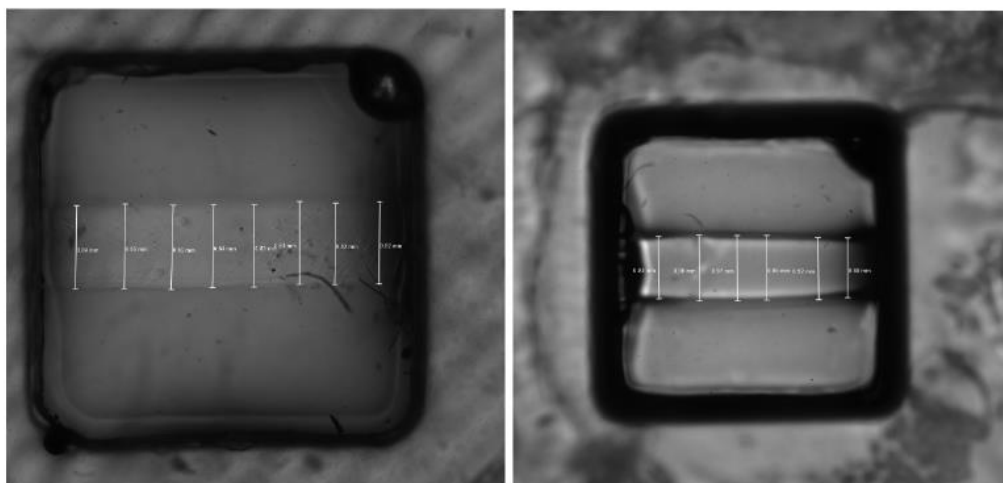


**Fig. 6. Selectively Crosslinked Hydrogel Channels.** This figure shows examples of the selectively crosslinked hydrogel material inside the wells of the device. These images depict results of photomasks with slit widths of 0.75 mm (left) and 1.0 mm (right). The widths depicted were made and measured using ImageJ software.

Photomask Channel Width (mm)	Average Hydrogel Channel Width (mm)	Standard Deviation (mm)	% Difference in Photomask and Hydrogel Channel Widths
0.50	0.543	0.0149	8.15
0.75	0.835	0.0119	10.73
1.00	0.94	0.0375	6.19
1.75	1.752	0.0426	0.10
2.00	2.027	0.0378	1.33

**Table 1. Selective Crosslinking Data.** This table shows the numerical data for the selective crosslinking experiment. Widths of the crosslinked hydrogel channels were determined using ImageJ software. The average width of the hydrogel channel that was formed was compared to the width of the photomask used, to determine the precision capabilities of UV crosslinking and the possible impact of light scattering.

indicate that culture within the device in granular hydrogel material is possible and successful.

#### *Selective hydrogel crosslinking using photomasks*

The feasibility of implementing additional features in our device for use in more complex applications was tested by the use of specially designed photomasks to selectively crosslink hydrogel using UV light to create microfeatures within the wells of the device. The photomask shape was chosen to represent the possibility of forming a channel made of crosslinked hydrogel through a well of the device. The results of this experiment are shown in Figure 6 and Table 1, where Figure 6 shows representative images of the solid hydrogel channels and Table 1 shows the numerical comparison between the intended feature width and actual feature width. This experiment successfully demonstrated that selectively crosslinking hydrogel using a photomask within the wells of our device can be done simply and

effectively. The possibility of creating standardized microfeatures out of hydrogel within our device is an important determination, as it proves that this device can be used in further research to create complex environments for cell culture to mimic native tissue and disease pathways. Additionally, this experiment demonstrates the importance of the essential design feature of a removable lid, which allows for manipulation of the material in the wells at any point in an experiment.

#### Discussion

The results outlined above confirm this device's ability to stabilize granular hydrogels during standard cell culture conditions while maintaining cell viability. In this way, Aim 1 was achieved. The success of selectively crosslinking hydrogel within the device using a specially designed photomask fulfills Aim 2. The removable lid of the final

device is essential to further applications of our device beyond simple, standard cell culture in granular hydrogels.

### ***Impact***

The design and prototyping in this capstone project have the potential to impact the field of tissue engineering and biomedical engineering by enabling long-term culture within granular hydrogels. By containing and stabilizing the material of granular hydrogels, researchers can more easily study the behavior of different cells in the dynamic environment presented by granular hydrogels. Furthermore, this device can help promote the development of more complex tissue and disease models. This device serves as a foundational and standardized method of studying granular hydrogels, aiding the formulation of tissue constructs. The use of granular hydrogels offers advantages over traditional bulk hydrogels, making them a promising alternative for various applications within the context of biomedical engineering, and our project enables others to help unlock their potential.

### ***Challenges & limitations***

There were several challenges and limitations faced throughout this research. Firstly, due to the time constraints of the project, only relatively short experiments of a few days were able to be performed using these devices. Cell viability and granular hydrogel containment results might be more effective or convincing in demonstrating the efficacy of this device. Additionally, there is a lack of quantitative data as a result of these experiments, partially owing to the nature of the project, but also due to issues with cell viability images. It is recommended that more experiments be conducted to quantitatively verify the results found in this project.

It is also important to note that since the components of this device are very small, they must be precise. Because of this, the technical capabilities of the 3D printers used to make the molds are very important. Some iterations and tests of the device were made using molds that were printed using FDM, and the results were imperfect and noticeably different from those made using SLA printing. This device is also limited in the volume of material it is able to hold. This may limit what experiments can be done using the device, but increasing the volume may be difficult as it could mean the mesh membrane would lack support. Another consideration is the reusability of the device. Because the lid can be removed, it is potentially possible to reuse the device by removing the contents by washing it with deionized water and resterilizing it in an ethanol bath

for 24 hours. However, this does not ensure that material did not seep between any of the layers or get stuck in a crevice of the device, and the reusability was not tested in this project.

Some technical issues with the device that may be limiting include the possibility of leakage through the lid, plasma bonding issues, and mesh slipping. Despite the testing done, there were still some minor issues with material leaking between the lid and the base. While no liquid escaped the device, at times there was some stuck between the lid and the base, creating a potential for contamination across wells of the device. Although plasma bonding was mostly successful in creating a strong bond between the PDMS base and the glass bottom, at times there were still some small sections that appeared to not be fully bonded. This is likely due to the imperfect surface of the PDMS base, as dithiol bonds require a very smooth surface. An air plasma cleaner was used, but a pure oxygen one may perform better in this situation to create a stronger bond. Additionally, testing the bond for longer durations of time is recommended to ensure its stability.

### ***Future work***

As tissue engineering continues to advance, the development of new devices for cell culture and tissue mimicry is essential. In this regard, the refinement of current devices is an ongoing effort that can significantly enhance the functionality and usability of the device. One area of improvement involves the incorporation of multi-channel systems that enable the perfusion of bioactive materials through the wells to elicit biological responses among cell populations. This enhancement can facilitate the creation of complex and dynamic systems that utilize granular materials and cell culture to accurately mimic native tissue.

Another promising area of development is bioprinting. The lid components of the device allow the system to be printed into and subsequently closed off to ensure material containment. Furthermore, researchers have access to the materials after bioprinting and can bioprint additional constructs or remove samples. The exploration of bioprinting can lead to the introduction of varying complexities in 3D-printed tissue constructs, which may lead to the creation of more physiologically relevant models for disease modeling and drug screening.

Selective cross-linking of the device is an area of exploration that could allow for more precise control over the mechanical properties of the hydrogel. The porous and



non-crosslinked nature of granular hydrogels offers a dynamic environment not found in bulk hydrogels. By utilizing selective cross-linking, a more tunable mechanical environment can be achieved. This approach could lead to cross-linked regions that are more akin to bulk hydrogels, while maintaining porosity, and potentially introduce new aspects in terms of cell motility and spreading throughout the material. This area of study could have implications for mimicking specific tissue types and understanding how cells respond to different mechanical environments.

Lastly, creating standardized protocols for designing and fabricating the device is essential to improve reproducibility across different labs and studies. This improvement would ensure the consistency and reliability of devices and results while utilizing them. The standardization of the protocol can help streamline the manufacturing process, reduce material usage, and increase efficiency, which are crucial factors for the scalability and adoption of tissue engineering devices.

## **Materials and Methods**

### ***Design and printing of device molds***

Devices were designed using the computer-aided design software SolidWorks. After the design was finalized, SolidWorks was used to create the negative of this design. This negative was 3D printed using a Formlabs Form 2 stereolithography (SLA) printer with their clear v4 resin, creating the molds. Throughout the design process, some of the initial iterations of molds were printed using fusion deposition modeling (FDM) printing, however, it was found that using this method produced molds with imperfections in the small features of the devices. SLA printing allows for more precision when printing very small features, proving to be better suited for manufacturing such a device.

### ***Fabrication of PDMS components***

To create the PDMS (polydimethylsiloxane) mold, Sylgard™ 184 silicone elastomer base was mixed with Sylgard™ 184 silicone elastomer curing agent at a weight ratio of 10:1. The mixture was stirred vigorously for approximately 3 minutes to ensure complete mixing of the two components. The mixture was then degassed using a VACUUBRAND ME1C vacuum pump at a suitable pressure until all air bubbles were removed. To speed up this process, the vacuum was turned off every 10 minutes to release any trapped air bubbles and then turned back until all air pockets were removed. The mold was then coated with PTFE Release Agent Dry Lubricant (MS0122AD) and allowed to dry for 15 minutes. The PDMS mixture was then

poured into the mold and placed in an oven set to 70°C for approximately 1 hour and 15 minutes or until the PDMS was fully cured. The mold was then removed using a lab spatula.

### ***Plasma bonding***

To plasma bond the glass coverslip, a Harrick Plasma Basic Plasma Cleaner was utilized. Prior to bonding, the polydimethylsiloxane (PDMS) base was cleaned with isopropyl alcohol (IPA) and dried with compressed air. The glass coverslip was washed with deionized (DI) water and also dried with compressed air. Both pieces were then placed inside the device and subjected to the plasma cleaner set at "high" for approximately 2 minutes. Once the plasma cleaning was completed, both pieces were immediately firmly pressed together, and pressure was applied for 1 minute.

### ***Cell and microgel staining***

Cell viability without the microgels was assessed using two different staining protocols. Human umbilical vein endothelial cells (HUVECs) were stained with DsRed and visualized, while fibroblasts were stained with LIVE/DEAD™. In the microgel and cell viability experiment, fibroblasts were stained with phalloidin and DAPI. The PEG microgels were tagged with fluorescein isothiocyanate (FITC) for visualization. The staining protocols described in Claxton et al. were used.

### ***Imaging***

Images were taken using an Olympus FV1000 confocal microscope.

### ***Photomask design and implementation of selective crosslinking***

Photomasks were designed using the computer-aided design software SolidWorks. The designs chosen for printing were made to sit securely on top of a single well of the PDMS device, with a slit of a specified width over the center of the well to allow light through, as depicted in Figure S2. Five photomasks were 3D printed using FDM printing, with slit widths of 500 µm, 750 µm, 1 mm, 1.5 mm, and 2 mm.

To test the photomask design, first a solution of norbornene-modified hyaluronic acid (NorHA) with a molecular weight of 90 kDa was mixed at a 3 wt% concentration with dithiothreitol (DTT) and a photoinitiator lithium phenol (2,4,6-trimethylbenzoyl) phosphinate (LAP). The degree of modification, or how many norbornenes per repeating

disaccharide unit in the HA backbone, was 0.3. About 160  $\mu\text{L}$  of this solution was pipetted into a well of the device. A photomask was then placed on top, and then the device was irradiated with 365-395 nm wavelength light at an intensity of 5  $\text{mW}/\text{cm}^2$  for 5 minutes. After this, the photomask was removed and the well was washed out by gently pipetting water in and out of the well, to remove the remaining uncrosslinked hydrogel precursor. The wells with crosslinked hydrogel features were then imaged using microscopy.

ImageJ software was used to determine the width of the crosslinked section at various points along the well. These values were averaged and compared to the width of the photomask slit to determine the percent difference between the two measurements and the standard deviation.

## **End Matter**

### ***Author Contributions and Notes***

Goedert, J. and Burnside, A. created CAD designs, constructed prototypes, performed experiments and analysis, and wrote the final report. Highley, C. advised on device designs and experimental procedures. The authors declare no conflict of interest.

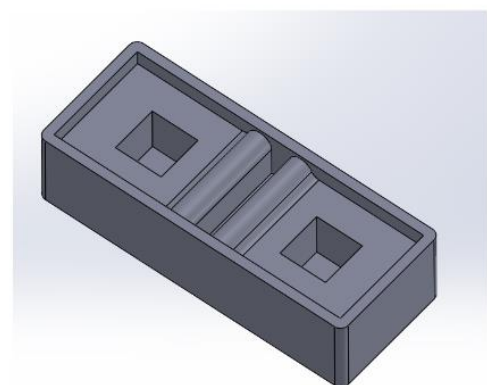
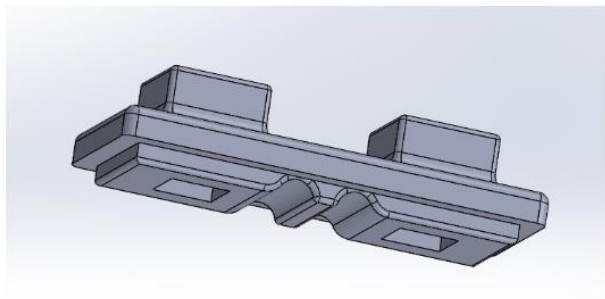
### ***Acknowledgments***

Natasha Claxton helped perform cell viability and microgel encapsulation experiments. Various members of the Highley lab at the University of Virginia helped test and provide feedback on device designs.

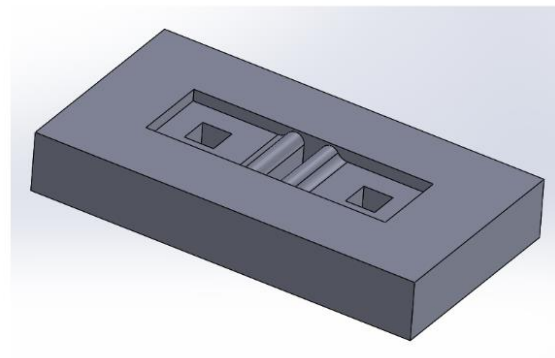
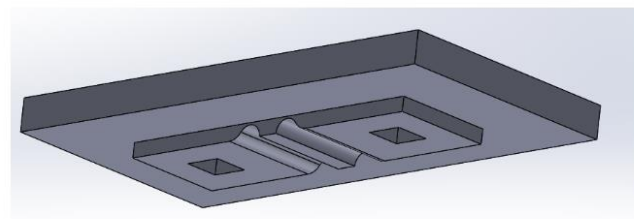
## **References**

1. Bashir, S., Hina, M., Iqbal, J., Rajpar, A. H., Mujtaba, M. A., Alghamdi, N. A., Wageh, S., Ramesh, K., & Ramesh, S. (2020). Fundamental Concepts of Hydrogels: Synthesis, Properties, and Their Applications. *Polymers*, 12(11), 2702. <https://doi.org/10.3390/polym12112702>
2. Claxton, N. L., Luse, M. A., Isakson, B. E., & Highley, C. B. (2023). *Engineering Particle-based Materials for Vasculogenesis* (p. 2023.03.15.532817). bioRxiv. <https://doi.org/10.1101/2023.03.15.532817>
3. Chai, Q., Jiao, Y., & Yu, X. (2017). Hydrogels for Biomedical Applications: Their Characteristics and the Mechanisms behind Them. *Gels*, 3(1), Article 1. <https://doi.org/10.3390/gels3010006>
4. Fisher, M. B., & Mauck, R. L. (2013). Tissue engineering and regenerative medicine: Recent innovations and the transition to translation. *Tissue Engineering. Part B, Reviews*, 19(1), 1–13. <https://doi.org/10.1089/ten.TEB.2012.0723>
5. Qazi, T. H., & Burdick, J. A. (2021). Granular hydrogels for endogenous tissue repair. *Biomaterials and Biosystems*, 1, 100008. <https://doi.org/10.1016/j.bbiosy.2021.100008>
6. Song, H.-H. G., Rumma, R. T., Ozaki, C. K., Edelman, E. R., & Chen, C. S. (2018). Vascular tissue engineering: Progress, challenges, and clinical promise. *Cell Stem Cell*, 22(3), 340–354. <https://doi.org/10.1016/j.stem.2018.02.009>

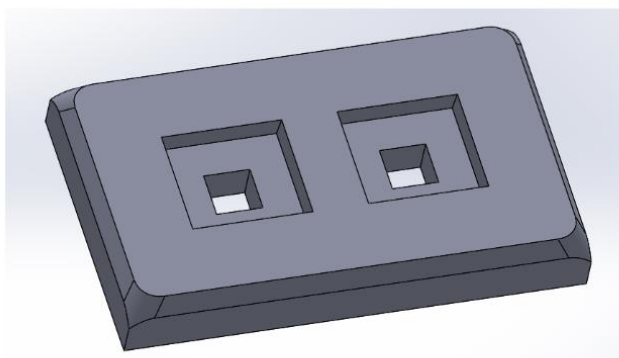
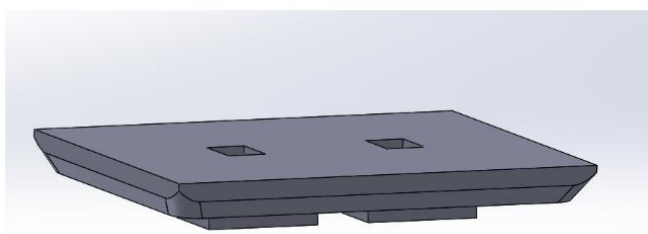
**Supplemental Material**



Lid (top) and base (bottom) version 1

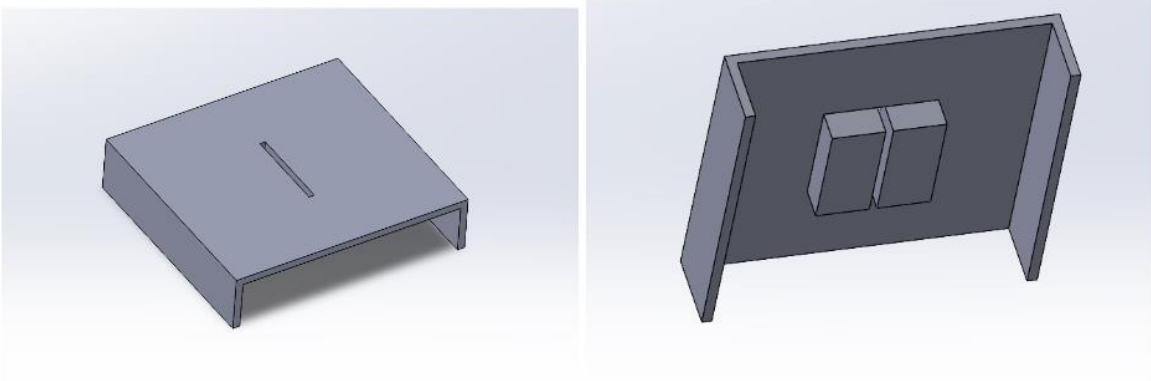


Lid (top) and base (bottom) version 3



Lid (top) and base (bottom) version 5

**Supplementary Fig. 1. Device iterations.**  
CAD models of early device iterations.



**Supplementary Fig. 2. Photomask design.** CAD models of final photomask design.